Journal of Membrane Science and Research 7 (2021) 141-151

Journal of Membrane Science & Research

journal homepage: www.msrjournal.com

Research Paper

Petroleum Refinery Wastewater Treatment Using a Polysulfone-Nano TiO_2 Hybrid Membrane Coupled with an Ozonation Process as a Pre-Treatment

Iwan Ratman [1], Tutuk Djoko Kusworo [2,3,*], Dani Puji Utomo [2]

[1] *Petro TNC International, Ltd., Equity Tower, 35th Floor Sudirman Central Business District (SCBD) Lot 9. Jl. Jend. Sudirman Kav. 52-53, Jakarta Selatan, 12190, Indonesia*
[2] *Department of Chemical Engineering, Faculty of Engineering, University of Diponegoro, Semarang, Indonesia*
[3] *Membrane Research Center (Mer-C), University of Diponegoro, Semarang, Indonesia*

Article info

Received 2020-01-20
Revised 2020-07-08
Accepted 2020-07-08
Available online 2020-07-08

Keywords

Fouling
Membrane
Ozonation
Petroleum
Refinery
Wastewater

Highlights

- The structural properties of PSf-TiO_2 membranes are presented.
- The influence of ozonation on membrane performances is investigated.
- Pre-treatment with ozonation significantly reduces fouling.
- Current challenges and coupled ozone-membrane treatment are discussed.

Graphical abstract

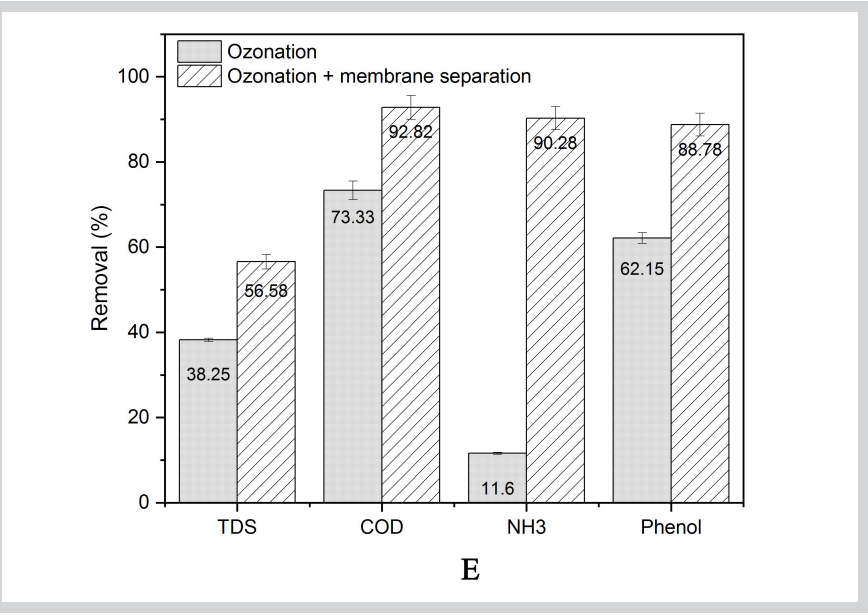

Abstract

Fouling has been the main problem that seriously hinders membrane applications for petroleum wastewater treatment. This study aimed to explore advanced membrane process integrated with ozonation as a preliminary treatment. Ozone utilization was set at a constant dose of 3000 mg/h for different ozonation times and temperatures. A longer ozonation time significantly improved the removal of pollutants. Ozonation at 30°C for 120 min removed up to 38.25% total dissolved solids (TDS), 73.33% organic compounds expressed as chemical oxygen demand (COD), 11.6% ammonia, and 62.15% total phenol. Although an increase in the ozonation temperature increased the ammonia removal by up to a remarkable 82%, it did not significantly affect the TDS, COD, and phenol removal efficiencies. Scanning electron microscope (SEM) and Fourier-transform infrared (FTIR) evaluations of the used membrane revealed that membrane fouling was caused by organic compounds consisting of hydrocarbon oil, benzene, toluene, xylene, phenol, and salt. Ozonation enhanced the permeate flux of the membrane by up to 96% and improved pollutant removal by up to 77%. The ozonation process was also responsible for the reduction of fouling resistance on the membrane surface by up to 21%.

1. Introduction

To convert the crude oil into usable refined products, petroleum refineries require complicated processes that generate a large volume of wastewater, typically 0.4 – 1.6 times of the volume of oil produced [1]. Effluent water in the petroleum refinery industry is produced through different typical processes such as separation, cracking, reforming, washing, topping, and lubing. Generally, these processes consume 246–340 liters of water per barrel of processed crude oil [2]. Petroleum refinery wastewater (PRW) contains complex pollutants, such as petroleum hydrocarbons, phenolic compounds, aromatic derivatives, heavy metals, ammonia, naturally occurring radioactive material (NORM), and other hazardous compounds [3]. Due to the hazardous contaminants in PRW, application of an appropriate wastewater treatment becomes important to reduce serious threats to the environment in terms of

* Corresponding author:E-mail address: tdkusworo@che.undip.ac.id (T.D. Kusworo)
DOI: 10.22079/JMSR.2020.120097.1332

living organisms, including aquatic lives and human health [4]. Appropriate wastewater treatment strategies are then required to achieve effective and cost-efficient processes for PRW pollutant removal.

Commonly, petroleum refineries generate wastewater that may contain various physical, chemical and biological contaminants in the form of salts, refractory organics, volatile compounds, heavy metals, dissolved gas, dissolved solids, dispersed oil, and biological pathogens. Over the last few decades, several wastewater-treatment technologies have been employed to reduce contaminants in PRW to their acceptable levels. To achieve better performance, wastewater-treatment technologies which include adsorption [5], coagulation [6], ion exchange [7], electrochemical separation [8], oxidation [9], biodegradation [10], and membrane separation [11] have been extensively studied for treating PRW. Although some of these technologies are effective in removing specific contaminants, they may not be effective in removing other types of pollutants in wastewater. Single physical PRW treatment, such as adsorption has been conducted by Fadali et al. [12] employing activated carbon, natural clay, and sawdust as adsorbents. They found that natural clay exhibits the best performance in adsorbing oil from wastewaters. Demirci et al. [13] used Al_2SO_4, $FeCl_3$, $FeSO_4$, and lime as coagulants as well as polyelectrolytes as coagulant aids and various types of clays to clarify the PRW in Turkey and successfully reduced the organic and suspended contaminants by as much as 90%. However, these techniques would not be effective on the other types of contaminants; moreover, for large-scale treatments, the solid waste created by spent adsorbents and chemical sludge needs further complicated treatments. In the recent years, the advanced oxidation and electrochemical have gained remarkable attentions in wastewater treatment [14]. Azizah et al. [15] developed an AOP using a combination of H_2O_2, ozone, and UV irradiation for treating residual fluid from catalytic cracking in the refinery industry. As expected, their proposed AOP effectively removes up to 93.75% of phenolic compounds. Brillas et al. [16] combined the Fenton process with electrochemical methods to effectively reduce an organic contaminant by converting it into CO_2, H_2O, and inorganic ions through the introduction of Fe^{2+} ions. However, this method failed to remove inorganic contaminants; moreover, the introduction of Fe^{2+} ions triggers new contaminations. The advanced physical separation method, such membrane separation using membrane, exhibits a wider range separation performance from particulate to molecular separation. However, membrane applications for wastewater treatment are limited by fouling, which may shorten membrane's life span and productivity.

Many researchers have reported their investigations to improve the anti-fouling behavior of polymeric membranes for water and wastewater treatment. The anti-fouling property of the membrane is usually enhanced by the improvement of hydrophilicity, wettability, electrostatic properties, decreasing the roughness, and surface tension of the membrane [17,18]. Various modification techniques, such as polymer blending with inorganic material, nanoparticle incorporation, surface modification (UV irradiation or plasma exposure), cross-linking, polymer coating, and surface functionalization, have been developed. Kusworo and his co-workers [19] fabricated the nano-hybrid PES membrane with SiO_2 and ZnO nanoparticle incorporation to improve membrane's performance and anti-fouling capacity. Seman et al. [20] reduced the fouling formation rate of the membrane through a UV-initiated graft polymerization. Later, Correia et al. [21] utilized a plasma treatment to enhance the wettability of PVDF membrane. Kim et al. [22] developed new membrane materials by modifying the membrane surface with silane coupling agents functionalized with specific structures to improve the fouling resistance. Unfortunately, these techniques are less effective when they are used to treat high organic content wastewater, such as PRW.

In this study, the combination of oxidation process and membrane separation were used for PRW treatment. Oxidation treatments were performed by injecting the wastewater with ozone generated by an ozonizer. The ozonation process was targeted to degrade the organic compounds, such as petroleum hydrocarbons, benzene, ethylbenzene, toluene, and xylene (BETX), phenolic compounds, and NH_3-N into simpler inorganic compounds. In this study, ozonation was utilized as a pre-treatment for PRW and followed by membrane filtration. The oxidized feed wastewater was then filtrated using a nanohybrid membrane consisting of PSf-TiO_2 nanoparticles. Basically, the membrane separation is responsible to the removal of dissolved contaminants, such as refractory compounds, NH_3-N, and inorganics ions. The PSf-based membrane was selected due to its advantageous physical properties, robust, chemical resistance, high thermal stability, and flexibility. The TiO_2 nanoparticles were embedded into the PSf membrane to improve membrane performance, following Kusworo and co-workers [23]. The combination of pre-ozonation and titanium dioxide nanoparticle incorporation into the PSf membrane is expected to give excellent performance in removing pollutants from PRW and reduce the fouling tendency. The structural properties, permeation and rejection performances, and fouling mitigation shown during PRW treatments were evaluated in this study.

1.1. Ozonation in wastewater treatment

Being an allotrope of oxygen comprised of three atoms of oxygen, Ozone is a relatively unstable and reactive gas. Therefore, ozone occurs naturally at deficient concentrations in the troposphere. The highest ozone concentration level is found in the stratosphere, which is about 6 ppm [24]. Because ozone is a commercially demanded treatment, there are four recognized methods for producing ozone from the air: corona discharge, ultraviolet radiation, electrolysis, and radiochemical treatment. The high reactivity of ozone is resulted by its inherent instability, which, in turn, comes from the molecule's readiness to accept an electron from an electron donor, which is then oxidized. The redox potential for ozone to induce a redox reaction is found to be 2.07 V [25].

Commonly, there are two different pathways of reaction involving ozone, namely, the indirect and direct reaction pathway, as shown in Figure 1(a). An indirect reaction depends on the radicals generated by the reaction between the ozone and an initiator, typically in the form of OH^* radical. The hydroxyl radical is highly unstable and reacts with electron-dense clusters in other molecules, such as amine, pi bonds, and aromatics. Hydroxyl radical formation depends on the pH of the system. The reactions of indirect pathways are numerous and very complex. However, such reactions can be represented by Eq. 1.

$$3O_3 + OH^- \rightarrow 2OH^* + 4O_2 \quad (1)$$

In contrast to the indirect pathway, the direct pathway is a much slower reaction. In a direct pathway, ozone reacts selectively with nucleophilic functional groups. For example, an ozone reaction with a double bond creates ozonide through complex reaction steps. The redox environment will determine the type of reaction products; an oxidative environment will produce ketone and a carboxylic acid; while a reductive environment will produce ketone and aldehyde, as shown in Figure 1(b).

It is crucial to consider that environmental conditions, such as pH, temperature, and the presence of oxidator, control the reactions pathways for system involving ozone. In wastewater treatment, ozonation is usually aimed to effectively oxidize the harmful materials, such as the decompositon organic materials into inorganic ions or gasses. For example, the oxidation reaction of ozone with N-NH_3 is presented in Eq. 2.

$$NH_3 + 4O_3 \rightarrow H^+ + NO_3^- + 4O_2 \quad (2)$$

The reaction rate for ammonia oxidation in water will be faster when the ozonation is performed under alkaline conditions (pH > 7) due to the presence of the hydroxyl group. The solubility and life-time of ozone in water are strongly temperature dependent. The solubility of ozone in water decreases at a higher temperature and is less stable. As expected, an increase of temperature enhances the reaction rate. Therefore, a study of the influence of temperature on the ozonation effectiveness in wastewater treatment is necessary. The introduction of ozone into wastewater is usually performed by a sparger or injector in the form of microbubbles to increase the stability and life-time of ozone in water.

2. Material and methods

2.1. Materials

Polysulfone (PSf) UDEL® PSU was purchased from Solvay Advanced Material Co. (USA). N-methyl-2-Pyrrolidone (NMP) as polymer solvent was procurred from Merck (USA). TiO_2 nanoparticles was synthesized in Nano Center Indonesia, (Indonesia). Ozone generator from Hanaco ozonizer (China) was used to produce ozone gas. Original PRW (the characteristics are presented in Table 1) was sampled from the outlet point of the primary wastewater treatment plant (WWTP) in Pertamina, Ltd. (Indonesia).

2.2. Fabrication of pristine PSf and nanohybrid PSf-TiO_2 membranes

The pristine PSf and nanohybrid membranes were prepared using the NIPS methods used in a previous study [26,27]. In particular, 0.5 wt% of TiO_2 nanoparticles were dispersed in NMP and blended with a polymer solution containing 19 wt% of PSf, 2 wt% of PEG and NMP as the solvent. The film was cast using casting tool onto a cleaned glass plate with an outlet gap thickness of 150 µm. The polymer thin film was coagulated via dry-phase inversion for 60 s, immersed in demineralized water at ambient temperature for wet-phase separation process.

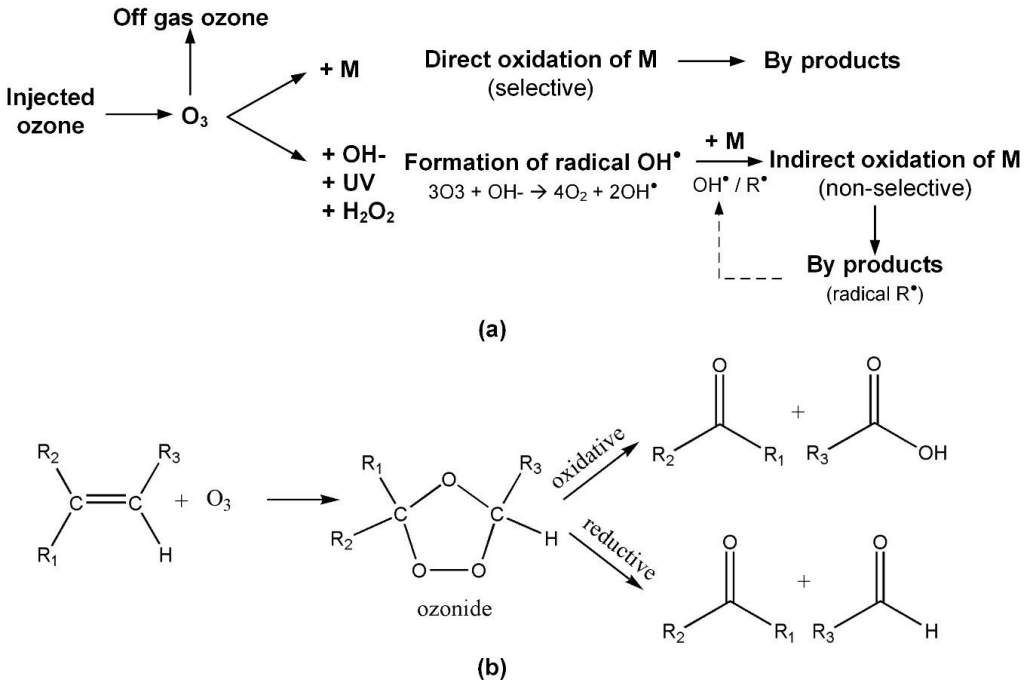

Fig. 1. (a) Schematic diagram of the ozone reaction pathway, (b) Example of direct ozone reaction pathway with double bond hydrocarbon.

Table 1
Characteristics of the PRW from Pertamina Ltd., Indonesia.

Parameter	Value
pH	7.6 – 8.0
Water turbidity, NTU	30 – 40
Organic expressed as COD, mgL^{-1}	650 – 1,000
Salts expressed as TDS, mgL^{-1}	1,000 – 2,000
Total phenol expressed as phenol, mgL^{-1}	50 – 150
Ammonia (as total N-NH_3), mgL^{-1}	25 - 100

2.3. *Membrane surface and cross-section morphologies*

The fabricated membranes were characterized to investigate the surface and cross-section morphologies using SEM (JEOL JSM-6510-LA, Japan). The membranes were cleaned using ethyl alcohol and dried at room temperature. For cross-section scanning purposes, the membrane was immersed in liquid N_2 to make it breakable. Membrane sample was then splitted using tweezers. The membrane sample was sputtered using pure gold and membrane structure images were captured under a certain magnification (5,000x and 20,000x for surface and 500x and 1,000 for cross-section).

2.4. *Ozonation and membrane filtration for PRW treatment*

The schematic system for the experimental equipment is presented in Figure 2. Continuous generation of ozone was facilitated by an ozonator at an injection rate of 3000 mg O_3/h. The ozone gas was injected into PRW feed water through a gas sparger. The total PRW volume in the feed tank was approximately 5 L. A piece of the tested nanohybrid membrane (with an effective surface area of 0.00159 m^2) was used in the cross-flow membrane filtration set-up. The ozone was injected into the wastewater prior to the membrane separation at a constant dose of 3000 mg/h. The injection was initially conducted for 30, 60, 90, and 120 min at a controlled temperature. The ozonated wastewater was then delivered to the membrane filtration under 5 bars of pressure. Prior to the PRW filtration experiment, the membrane was pre-compacted using demineralized water at 5 bars of pressure for 0.5 h. The PRW water was pumped to the membrane cell, and the trans-membrane pressure was maintained at 5 bars by regulating the outlet valve of the retentate stream. The volumetric feed flowrate of the PRW during filtration process was 1.0 L/min. The PRW filtration using membrane was performed for 150 min (2.5 h), whereas the membrane stability test was performed for 8 hours. The permeate water was collected over a period of time, and the retentate water was circulated to the feed tank. The permeate water flux (J) was calculated using Eq. 3 as follows [28].

$$J = \frac{V_i}{A \times \Delta t} \tag{3}$$

where V_i is the permeate volume collected during filtration (L), A is the effective membrane area, (m^2), and Δt is the time in which the permeate was collected (h).

The evaluation of pollutant removal, as well as the analysis of contaminant concentrations in both upstream and downstream water were performed. The TDS was directly measured using a TDS-meter (Hanna TDS meter, UK). The COD in the feed and permeate were determined using the dichromate digestion method via Test Tube Heater-COD Reactor (HANA HI 839800, UK) for 2 hours at 150°C; the trivalent dichromate was measured using a spectrophotometer (Perkin Elmer Lambda 20, US) at wave length of 600 nm. Total phenolic compounds were examined using phenol test kit (Hanna Instrument HI 3864, UK). For ammonia determination, the sample was reacted with Nessler reagent, and the colored solution was measured using a spectrophotometer (Perkin Elmer Lambda 20, US) at wave length of 525 nm. The turbidity of wastewater was measured using a nephelometer. The methods were adopted from Indonesian standard analysis for wastewater (SNI 06-6989.30-2005). The pollutants rejection efficiencies were calculated using Eq. 4 as follow [29]:

$$\%R_i = \left(1 - \frac{C_{pi}}{C_{fi}}\right) \times 100\% \tag{4}$$

where C_{pi} and C_{fi} are the concentrations of the contaminant/solute in the permeate and feed water, respectively.

2.5. *The qualitative and quantitative analysis of membrane fouling*

The qualitative analysis of fouling in the membrane was performed using SEM and FTIR analysis. The surface of the fouled membrane was sputtered using pure gold to improve conductivity. Then the membrane sample was observed under a certain magnification (10,000× and 20,000×). The fouled surface of the membrane with ozonation pre-treatment was compared with the

fouled surface of the membrane without pre-ozonation. The identification of foulant compounds on the membranes was performed using FTIR spectrophotometer (Perkin Elmer Frontier, USA). The FTIR spectra of fouled and clean membranes were recorded in the range of wavenumbers of 400 to 4000 cm^{-1}. These characterizations were performed to investigate the type and amount of foulants deposited on the membranes' surfaces and internal layers.

The quantitative analysis of membrane fouling was performed using the pure water flux decline ratio and membrane resistance measurements. Permeate flux decline is caused by the formation of fouling and concentration polarization in the membrane during the PRW filtration process. In this study, only the flux decline caused by foulant deposition was observed. The flux declines were determined according to Eq. 5 and 6 [30].

$$RJ_T = \frac{J_0 - J_S}{J_0} \times 100\% \quad (5)$$

$$RJ_f = \frac{J_0 - J_f}{J_0} \times 100\% \quad (6)$$

where RJ_T and RJ_f are the total flux decline, and flux declined caused by fouling, respectively; J_0 is the pure water flux of the clean membrane; J_S is the wastewater permeate flux; and J_f is the pure water flux of the fouled membrane.

A series resistance model derived from the Darcy equation was used to evaluate the membrane resistance during refinery wastewater treatment in this study. The pure water permeation method was used for evaluating the membrane resistance. The resistance in membrane filtration comes from the membrane structure (intrinsic factor), irreversible fouling (absorbed foulant), and reversible fouling (cake formation on the membrane surface). R_m, R_a, and R_c were determined according to Eq. 7 – 10, as follows [31].

$$R_m = \frac{\Delta P}{\mu \times J_0} \quad (7)$$

$$R_a = \frac{\Delta P}{\mu \times J_a} - R_m \quad (8)$$

$$R_c = \frac{\Delta P}{\mu \times J_f} - R_m - R_a \quad (9)$$

$$R_T = R_m + R_a + R_c \quad (10)$$

where R_m, R_a, and R_c are the resistances of the membrane, absorbed foulant, and cake formation, respectively (m^{-1}); μ is the viscosity of pure water at 25°C (8.90 x 10^{-4} Pa.s); J_0, J_a, and J_f are the pure water fluxes for the clean membrane, membrane with absorbed foulant, and fouled membrane, respectively ($m^3.s^{-1}$); and ΔP is the upstream pressure applied to the membrane during the permeation test (Pa).

3. Results and discussions

3.1. Morphologies of the fabricated membrane

The surface and cross-sectional structures of the fabricated membranes are evaluated to investigate the separation properties of the membrane. Figure 3 presents the membrane morphological images of the PSf membrane with a 0.5 wt% TiO_2 nanoparticle concentration. The surface of the membrane is smooth, and no unselective void defects are observed. Because the membrane pores cannot be observed at 20.000× magnification, it can be assumed that the pore size of the membrane is at the nano-scale level. The white spots observed on the membrane surface might be the nanoparticles embedded in the PSf polymer. The presence of the TiO_2 in the PSf membrane can be confirmed by the XRD pattern as shown in Figure 4. The typical diffraction pattern of the TiO_2 was also appeared in hybrid membrane among the PSf diffraction pattern. The crystalline peaks at 27.47°, 36.25°, and 54.40° are analogous with dominant characteristic crystalline peaks of pure TiO_2 at 27.27°, 36.06°, and 54.26° as reported by Wu et al. [32]. There were very few nanoparticles observed on the membrane, which could be due to the low concentration level of nanoparticles loading into dope solution used in this study, i.e., 0.5 wt%. Another possible phenomenon is that the nanoparticles are embedded under the skin layer of the membrane. Small quantity of nanoparticle clumps were observed on the surface of the PSf-TiO_2 0.5 wt% membrane. Therefore, the absence of unselective void around the nanoparticle indicates that the TiO_2 particles are uniformly attached to the polymer. As reported in the previous study, the rougher membrane resulting from nanoparticle agglomerates is usually found as the TiO_2 loading is more than 0.5 wt% [33]. The existence of agglomerates is not favourable in membrane preparation due to a higher membrane fouling tendency, and in some cases, the agglomerates reduce the separation properties.

Figure 3C and D show the cross-sectional image of the prepared membrane at 500× and 1,000× magnification. This typical asymmetric structure consust of a dense layer, finger-like micropores, and a sponge-like base. The pores with the finger-like structures extend from near the surface to the bottom of the membrane. The finger-like structures provide the permeability properties of the membrane. These structures are formed during the water-induced coagulation process due to the migration of the solvent (NMP) and other water-soluble materials from the polymer region to the non-solvent region.

3.2. Effect of ozonation time on pollutant removal

The ozonation experiments for PRW treatment were conducted in using constant ozone doses of 3000 $mg.h^{-1}$ for various injection times. The ozonation time is an important key in maximizing the pollutant degradation reaction due to the short life-time of ozone in water which is around 15 min at 298K and pH 7 [34]. However, some contaminant compound degradation reaction rates with ozone are slow. Figure 5 presents profiles of the removal efficiencies of various pollutants as functions of ozonation time.

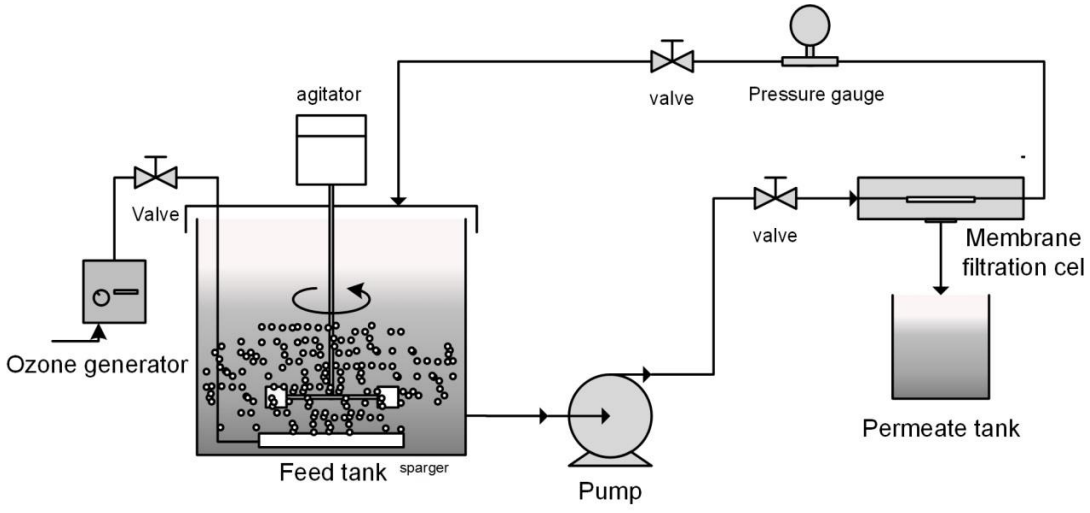

Fig. 2. Process diagram for membrane filtration with ozone as a pre-treatment.

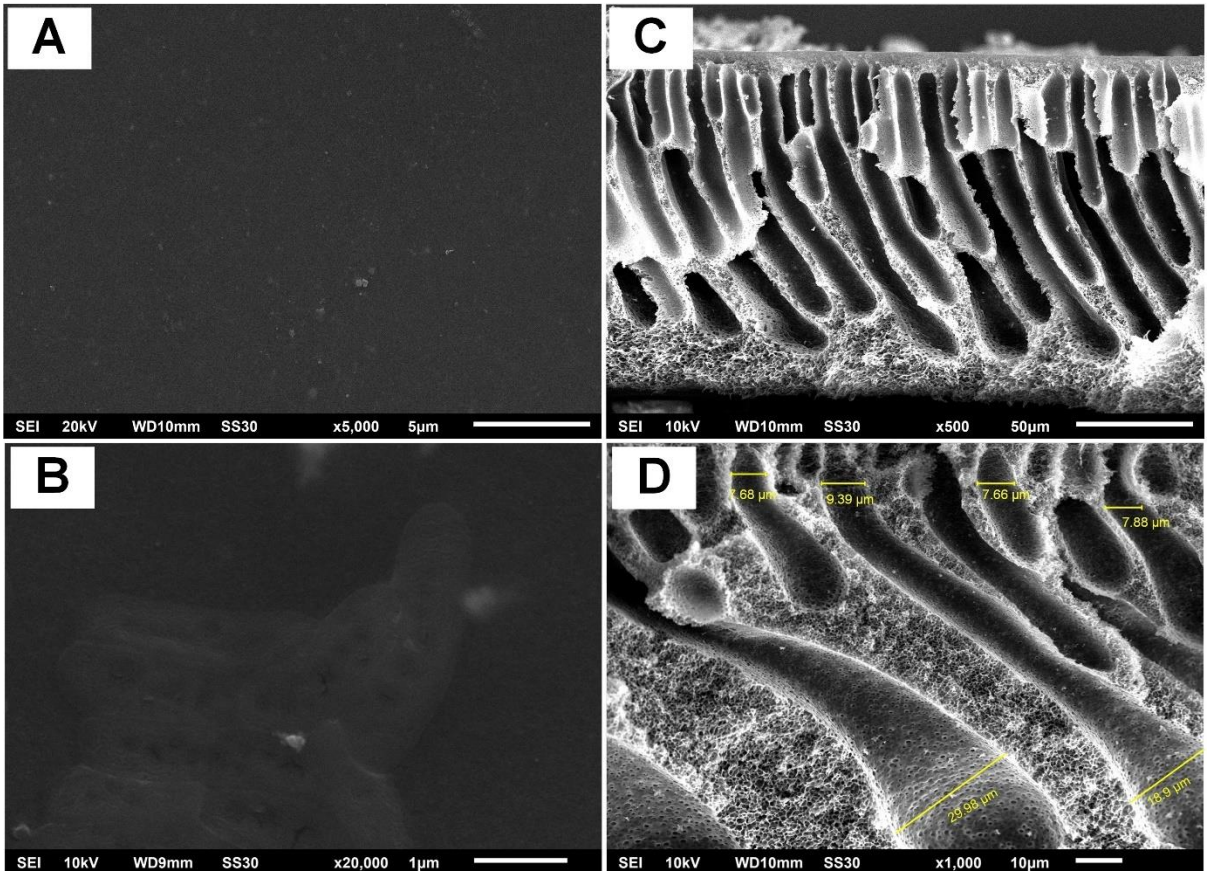

Fig. 3. SEM images of PSf-TiO_2 0.5 wt% membrane (A) and (B) surface morphologies at 5,000× and 20,000× maginification, (C) and (D) cross-section morphologies at 500× and 1,000× magnification.

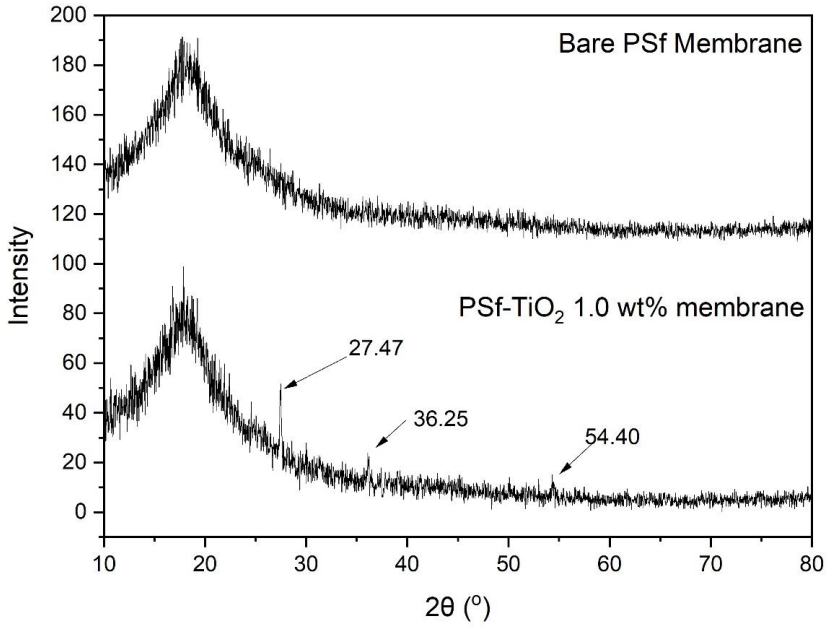

Fig. 4. XRD pattern of bare PSf membrane and nanohybrid PSf-TiO_2 1.0 wt% membrane.

Figure 5 depicts that in the first 30 min, phenol removal efficiency is the highest, and is followed by COD, TDS, and ammonia removal efficiencies. At this period of time, the removal efficiency for phenol, COD, TDS, and ammonia were 56.77%, 41.62%, 37.65%, and 3.84%, respectively. The higher removal efficiency of phenolic compounds could be due to their high reactivity with ozone. Phenolic compounds have a benzene ring with delocalized electron clouds. Moreover, the reaction occurs at an initial pH of 7.8. Under a slightly basic condition, phenolic compounds dissociate into phenolates ions, and such ions exhibit higher reactivity than phenol. Phenol decomposition via ozone begins through an electrophilic attack on the double

bonds in the benzene ring. The oxygen from the ozone molecules is attached to the ring to create a quinone compound. Further oxidation occurs in the presence of excess ozone, where the quinones decycle into organic acids in the oxidative environment and produce aldehyde in the reductive environment. Accordingly, an extended oxidation process should decompose the simple organic acids into CO_2 and H_2O [35]. These reaction pathways of phenol decomposition are summarized in the diagram depicted in Figure 6. After a 30-min ozonation process, phenol removal increased slightly, which could be due to the production of acid because acid lowers the pH and reduces the oxidation rate. Hence, the increasing removal of phenols as a function of time is not linearly proportional.

As shown in Figure 5, initial COD removal is relatively high although it is removed at a lower rate than phenol. COD represents the oxidized compounds in the wastewater, such as hydrocarbon oil, BTEX, organic acids, alcohol, ether, and refractories, such as NH_3-N, and sulfide. With an increase in ozonation time, the COD removal efficiency increases significantly. This removal efficiency enhancement can be attributed to the transformation of recalcitrant organic compounds into more reactive compounds during ozonation. The formation of hydroxyl radicals in the decomposition of alcohol is one such example. The TDS in wastewater is also reduced by ozonation at a 37% rate. TDS comprises the mineral ions from both metallic and non-metallic cations and anions. Some anions in water, such as Cl^-, Br^-, and OH^- can be oxidized (forming Cl_2, Br_2, O_2, and H_2, in the case of the anions listed herein); thus, the TDS in the water decreases. As the ozonation process progresses, the changes in TDS removal are insignificant. This result could be explained by the remaining minerals in the wastewater being cations and oxidized anions. Ammonia removal using ozonation exhibits the lowest removal efficiency, which could be due to the reaction rate in the NH_3-N decomposition via ozone being very slow (ozone life-time is about 15 min at 298K and pH 7) [34]. NH_3-N was oxidized into nitrate ions in water. The ammonia removal increases significantly after 60 min ozonation due to the reaction of ozone with ammonia involving multiple steps of reaction. Firstly, the ozone will generate the hydroxyl radical from the existing hydroxyl ion. If the hydroxyl level is not enough, ozone will produce hydroxyl ion from water or carbonate ion. Unfortunately, the reaction of ozone was also controlled by the gas-liquid interfacial mass transfer. Therefore, the longer the ozonation process increases the hydroxyl radical concentration; besides, the mass transfer rate of ozone to the liquid body is also higher and accelerates ammonia oxidation.

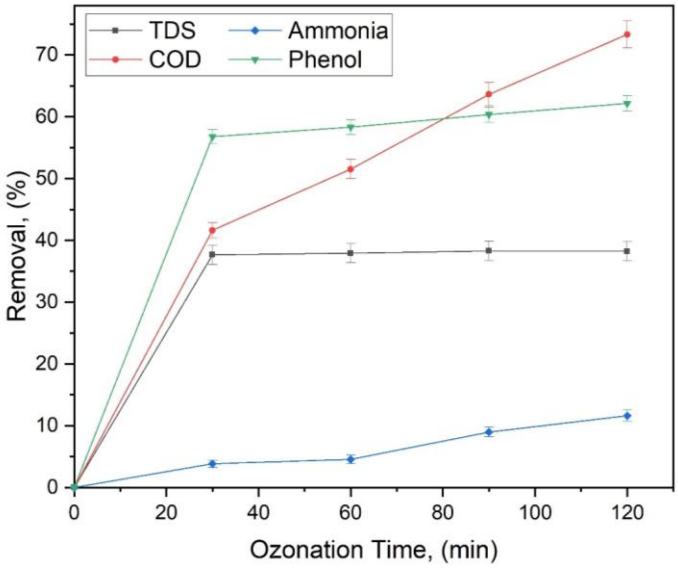

Fig. 5. Removal efficiencies of pollutants in PRW for various ozonation time.

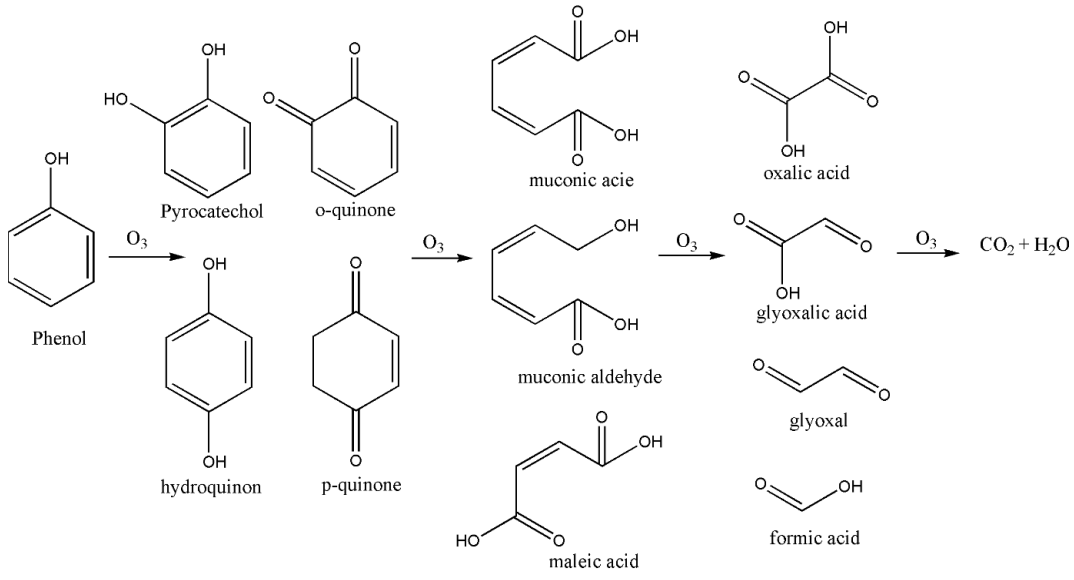

Fig. 6. The reaction pathway of phenol oxidation by ozone.

3.3. Effect of temperature on the ozonation process

The ozonation experiments were also conducted with different feed temperature. The temperatures were maintained at 25°, 30°, and 35°C with a constant ozonation dose of 3000 mg O_3/h for 120 min. The changes in pollutant removal efficiencies are shown in Figure 7.

As illustrated in Figure 7, temperatures does not significantly affect the TDS removal. The removal efficiency remains at the level of 37-38% for all temperatures. However, a slight removal enhancement is observed for COD removal. The removal efficiency increases from 73 to 76%. In addition, a slight increase in phenol removal efficiency at increased temperatures was also observed, which ranged 62 to 63.75%. As expected, significant improvement in NH_3 removal is exhibited, as the efficiency increases from 11.6 to 19.4 %.

The temperature strongly influences the solubility and stability of ozone in water. Theoretically, increasing of temperature increases the decomposition rate due to the kinetic energy enhancement. However, the solubility of ozone decreases with increasing temperature [36]. Both solubility and increasing reaction rates could affect ozonation efficiency, leading to organic contaminant removal efficiency changes. Based on this experiment, the changes in TDS removal at different temperature were negligible. The result is plausible because TDS consists of cations and anions, the metal cations can't be removed by oxidation, while some anions can be oxidized. The indirect oxidation reaction has higher activation energy than indirect oxidation [37] and most of the anion oxidation by ozone is indireact reaction for example the oxidation of Br^- to form Br_2 gas [36] and Cl^- conversion to Cl_2 [38], the higher activation energy causes the reaction becomes less temperature-depedent. For COD and phenol removals, an increasing temperature from 25 to 30° C shows a significant removal efficiencies enhancement, however at the higher temperature of 35°C; the removal increases are not significant. It could be due to at the initial temperature increment resulted in the enhancement of the the organics decompositions due to the enhanced kinetic energy, i.e., the compounds and ozone became more reactive. While, at a higher temperature, the solubility effect becomes more prominent. The solubility of ozone and the majority of gasses in water decrease as the temperature increases. With the decrease in ozone solubility, the residence time of ozone in water becomes shorter. A different phenomenon was observed in the removal of NH_3, whereby increasing the temperature increased the removal efficiency significantly. This increase in efficiency could be due to the presence of NH_3 in the water being in its equilibrium state of NH_3 and NH_4^+ions. As the temperature increases, the solubility of NH_3 decreases. Hence, the enhancement in the NH_3 removal efficiency is the result of not only by the ozone oxidation process but also by the release of NH_3 from water due to its decreased ammonia solubility as the result of temperature increase [39]. From this experiment, it can be concluded that an optimum temperature for ozonation process should exist to achieve maximum pollutant removal because an increase in temperature results in two opposites effects: an increase in kinetic energy for the reaction, but a decreases in ozone gas solubility.

3.4. Combination of pre-ozonation and membrane filtration for PRW treatment

The ozonation was used as a pre-treatment for membrane filtration. After ozonation for 120 min at 30°C, the wastewater was filtrated using the PSf-TiO_2 nanohybrid membrane. The permeate fluxes obtained from a single membrane filtration process and the combined ozonation and membrane filtration process are presented in Figure 8.

Declining permeate fluxes are observed for both processes, as presented in Figure 8. The decline in the permeate flux is a general phenomenon in membrane separation. The initial sharp decrease is usually attributed to the deposition of foulant on the membrane surface and membrane compaction. The deposition of the foulant greatly decreases the permeate flux. For longer filtration times, the profiles show that pseudo-steady state conditions are reached at 0.5 $Lm^{-2}.h^{-1}$ and 1.38 $Lm^{-2}.h^{-1}$ for single membrane process and pre-ozonated membrane processes, respectively. These results indicate the deposition of the adsorbed foulant on the membrane and concentration polarization on the membrane surface. Adsorbed foulants deposited in the internal membrane matrix and irreversibly attached. The increasing concentration of foulants around the membrane region causes the concentration polarization which leads to the flux decline. Overall, the combined system (ozonation as a pre-treatment) exhibits a higher permeate flux than the membrane-only system, which could be due to the result of the majority of the organics (almost 70% based on the COD removal as shown in Figure 9) being removed during the ozonation process. Organics are known to be the main cause of membrane fouling. Oil droplets, aromatics, and hydrocarbon derivatives have high affinities for hydrophobic surfaces such as PSf, which has a slightly hydrophobic nature. The ozonation process also exhibited an excellent performance in removing refractory organic compounds that usually cannot be treated completely by physical and biological treatments. Based on these results, the ozonation significantly enhances the membrane's permeate flux performance.

The Membrane's performance evaluation in terms of pollutant removal rates is shown in Figure 9. The pollutant removal rates obtained in the standalone membrane filtration mode were compared with those of the coupled ozone-membrane system. The coupled memrbane system as presented in this work significantly enhanced the removal efficiencies for all pollutants. The TDS removal was enhanced from 38.25 to 50.58%, the COD removal efficiency increased from 73.33 to 92.82%, the NH_3 removal was drastically enhanced from 11.6 to 90.28%, and the phenol removal efficiency improved from 61.15 to 88.78% with this approach. Hence, an enhancement in membrane permeability can be achieved without sacrificing the separation performance of the membrane.

The membrane alone removed just 38% of the TDS. This low removal efficiency is due to the presence of monovalent and multivalent ions. Nanofiltration is unable to reject monovalent ions, such as H^+, K^+, Na^+, Cl^-, and F^-. The removal of minerals is not controlled by the size exclusion mechanism, while the rejection of organic compounds, ammonia, and phenols is affected by both the size and Donnan exclusion mechanism. Larger molecular sizes and molecular electrostatic charges lead to higher removal efficiency for organic compounds compared to mineral. As presented in Figure 9, the rejection rate of NH_3 was greatly enhanced due to the effect of Donnan exclusion involving a similar electrostatic charge. The electrostatic charge TiO_2 is negative when the pH of the solution is above 6 [40], it caused the PSf membrane surface was negatively charged. In water, ammonia could be in the form of dissolved NH_3 or/and NH_4^+ ions based on the equilibrium equation $NH_3 + H_2O \leftrightarrow NH_4^+ + OH^-$. In the presence of OH^- (pH > 7) the equilibrium shifts towards NH_3, where NH_3 is a Lewis-base so it will be excluded by a negatively charged membrane surface. The pre-ozonation of PRW feed before membrane separation significantly enhanced the average permeate flux up to 96% and average pollutants rejection up to 77% compared to the standalone membrane filtration's performance. Suprisingly, the experimental results showed that improving the removal efficiency can be done without degrading the permeate flux performance.

3.5. Qualitative analysis of membrane fouling

Membrane fouling is related to the productivity of the membrane filtration where the presence of foulant on the membrane deteriorates its performance. The presence of fouling can be noticed by the significant decline of permeate volume as the operating time increases. In order to evaluate the fouling behaviour of the PSf-TiO_2 membrane, it was used in PRW treatments, with and without ozonation, and then a SEM analysis was carried out. The SEM images of the fouled membranes are shown in Figure 10.

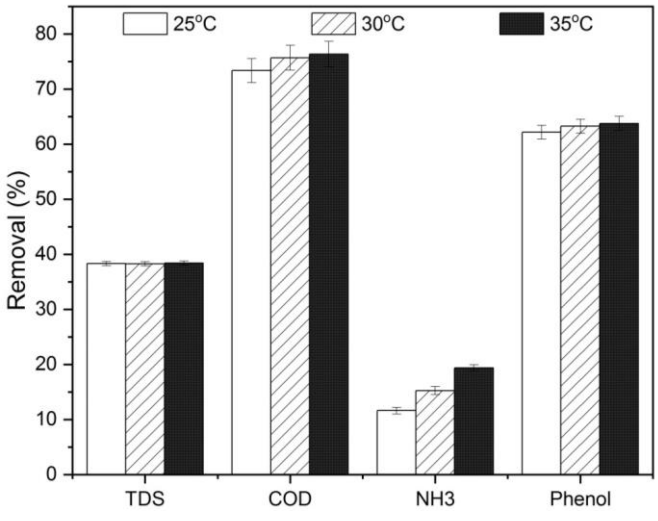

Fig. 7. Pollutant removal efficiencies at different temperatures.

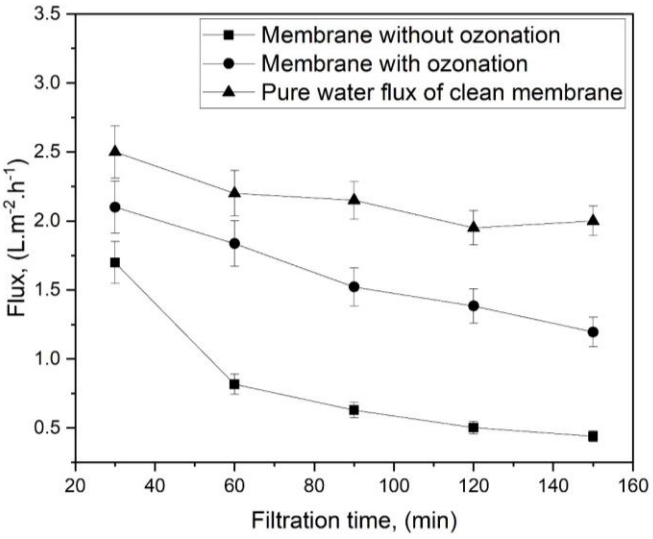

Fig. 8. The flux profiles for ozonation and membrane separation.

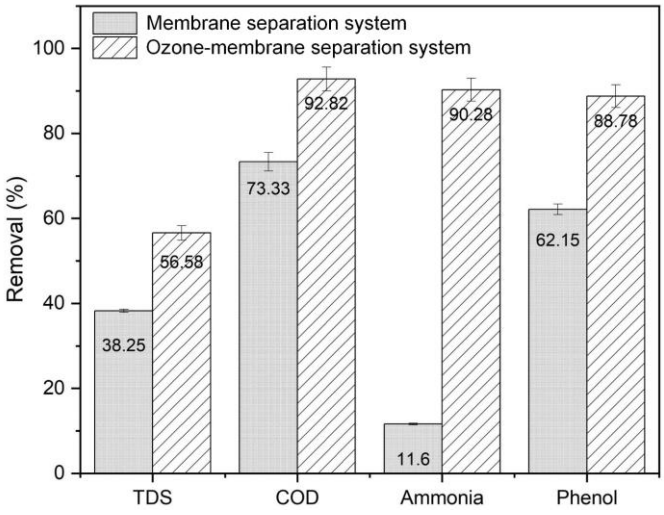

Fig. 9. The percentages of pollutants removal by the membrane separation system and ozone-membrane separation system

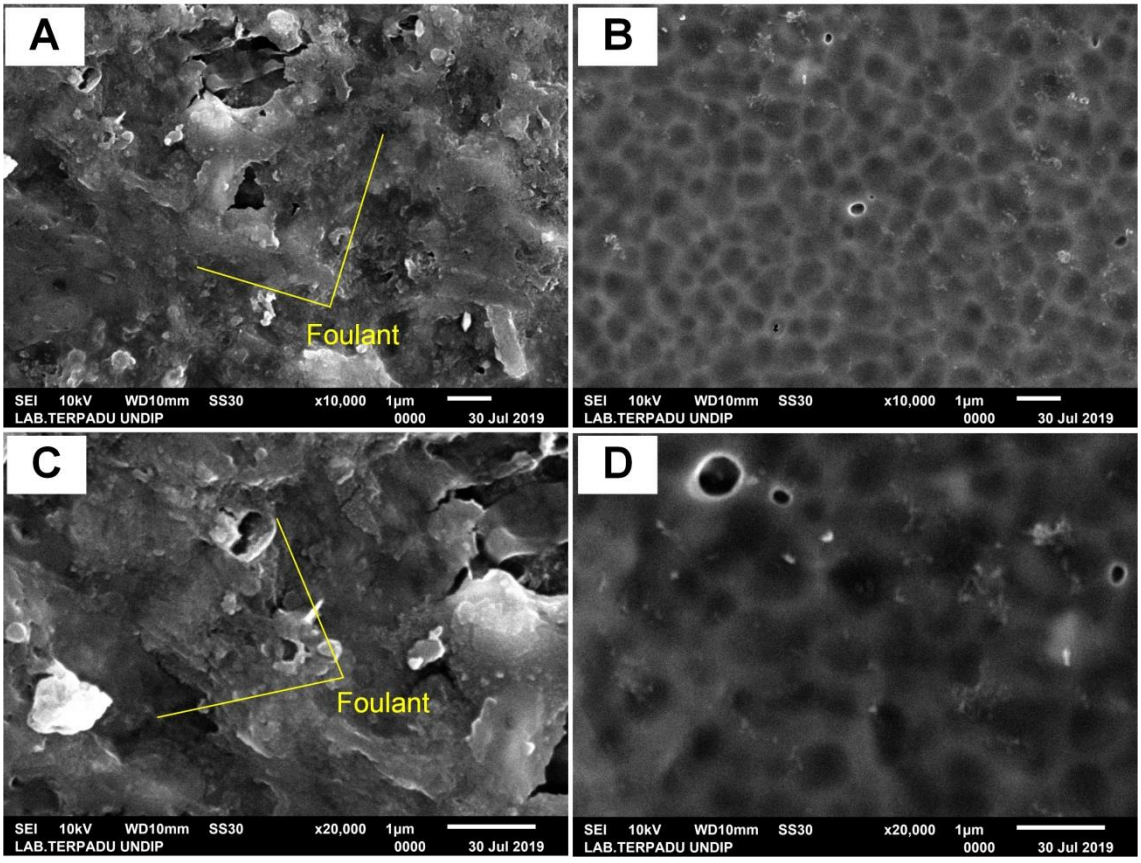

Fig. 10. SEM images of foulant deposition on the membranes, (A) and (C) show the fouled membrane scanned at 10,000x and 20,000x. (B) and (D) show the fouled membrane coupled ozonation as a pre-treatment scanned at 10,000x and 20,000x.

As can be seen in Figures 10A and C, the contaminants on the PSf-TiO_2 membrane without the ozonation process formed a massive organic cake. However, for the membrane accompanied by ozonation as a PRW pre-treatment in Figure 10B and D, the surface was cleaner, and only some particulates pollutants were found. The fouling layer on the PSf-TiO_2 membrane without ozonation as a pre-treatment was rougher compared with membrane with ozonation applied as a pre-treatment. These results support, and are also in accordance with, the fouling phenomenon decreasing the permeate flux during membrane filtration (as shown in Figure 8). The phenomenon of fouling formation during membrane filtration is commenced by the attachment of organic compounds or microorganism, which is then followed by the precipitation of inorganic matter or minerals as well as particulate fouling to form cake layer [41]. This mechanism explaines why the ozone-membrane system shows a reduced fouling layer on its surface. The ozonation process successfully removed about 73% (see Figure 9 for COD removal) of the organic matter in the wastewater. The accumulation of oil droplets on the membrane is usually the initiator of membrane fouling especially in oily wastewater [11].

Generally, pore-blocking by attached foulant initiates the phase of fouling growth mechanism as reported by previous works [41,42]. However, in this study, organic compounds were absorbed on the pore walls of the membrane and altered the superficial properties, which initiated further foulant deposition. Previous researchers have identified the type of fouling via the shapes or characteristics of the foulant deposits using SEM or FESEM image scanning [43,44]. Based on the types of foulant deposits shown in the SEM images, the membrane without the ozonation pre-treatment was fouled by organic compounds, while the membrane with the ozonation process was fouled by salts and particulates. Hence, it can be inferred that the ozonation process is responsible for reduced accumulation of organic foulants on PSf-TiO_2 membrane's surface.

FTIR spectra of clean and fouled PSf-TiO_2 nanohybrid membranes were also recorded as shown in Figure 11. The FTIR spectra for the clean membrane include the typical peaks for the Polysulfone backbone and functional groups. Peaks at 1240, 1585, 1490, and 1350 – 1300 cm^{-1} represent the ether bond (Ar-O-Ar), aromatic rings, methyl group, and sulfone (S=O) group, respectively. The fouled membrane exhibits quite different FTIR spectra in that the broad peaks from 3700 – 2000 cm^{-1} are larger, indicating that the major foulant on the membrane contains hydroxyl groups from alcohol, organic acids, and aldehyde. The stronger peaks at 1650 and 1585 cm^{-1} indicates the deposition of organics that contains aromatic rings such as phenolic, benzene, toluene, and xylene. The appearance of the band at 3100 cm^{-1} indicates double bond-containing organic compounds, and it may come from a benzene ring or an aliphatic alkene. The strong peaks at 1400 – 1050 cm^{-1} come from hydroxyl vibrations of phenolic compounds. It is concluded that the majority of organic foulants on the membrane are phenolic compounds, hydrocarbon oils, BTX, organic acids, and aldehydes. Although the typical peaks of foulant components are found in the both fouled membrane spectra, there are significant differences of peaks exist between the spectra of fouled membrane with ozonation (Figure 11B) and fouled membrane without ozonation (Figure 11C). The large peak of hydroxyl vibration (3700 – 2000 cm^{-1}) of the fouled membrane without ozonation exhibits lower transmittance signals compared to that of pre-ozonated membrane. This result indicates that there are more hydroxyl-containing foulants attached on the membrane without ozonation than ozonated membrane. It is noticed that the pre-ozonated membrane also shows higher IR absorption at 1750, 1650, and 1585 cm^{-1}, which are related to the aromatic ketone, aromatic CH, and amine bendings, respectively. The possible reason is that the aromatic foulants may come from the intermatdiate oxidized products of BTEX and phenolic such as quinone, benzoquinone, benzaldehyde, etc [45]. These compounds have higher affinity with polysulfone molecule than BTEX, thus there are higher aromatic foulant deposition of these compounds on the pre-ozonated membrane compared to that of unozonated membrane. However, there was a significant effect of pre-ozonation in decreasing the overall foulants deposition on the membrane as presented in the FTIR spectra.

3.6. Quantitative analysis of membrane fouling

According to Darcy's law of fluid transport through a porous barrier, the permeate flux is inversely proportional to the membrane resistance. When the permeate flux decline with filtration time in a membrane with operational conditions and feed held constant, this decline indicates increasing membrane resistance. This membrane resistance in membrane filtration is the result of an intrinsic membrane and fouling resistance. The fouling resistance may come from adsorbed fouling, reversible fouling with a cake formation, and concentration polarization. In this study, the membrane resistance created by intrinsic membrane resistance, adsorbed fouling, and cake formation was evaluated through the pure water permeation method. The results of this resistance evaluation are presented in Figure 12.

As shown in Figure 12, the intrinsic membrane resistance (R_m) has the same value for the membranes involved in the solo and combined processes since the same type of membranes was used in both cases. The resistance encountered due to adsorptive fouling and cake formation on the membrane without the ozonation process was greater than that for the membrane coupled with the ozonation process. The cake retention of the membrane with pre-ozonation is slightly higher than that of the membrane process alone. The reasonable answer to this phenomenon is due to the generation of metal hydroxide precipitate as a result of hydroxyl radical generation by ozone. However, the organic fouling resistance (absorbed foulant) can be reduced by up to 21% from 1.68×10^{16} m^{-1} to 1.33×10^{16} m^{-1} by ozonation for 120 min at 30°C prior to membrane filtration. This evaluation has disclosed a remarkable enhancement in fouling mitigation as a result of ozonation as a pre-treatment for PRW prior to membrane filtration.

4. Conclusions

In this study, acomparison of PSf-TiO_2 nanohybrid membrane filtration systems without and with an ozonation pre-treatment was made. The ozonation time significantly increased pollutant removal in terms of COD, phenolic, and ammonia removal efficiencies. The best ozonation results occurred when ozonation was conducted for 120 min at 30°C. At higher temperatures, the enhancement was not significant due to the equilibrium in ozone solubility and residence time of ozone in water. The ozonation treatment was shown to improve the flux in membrane separation by up to 96% and pollutant removal by up to 77%. Meanwhile, the ozonation pre-treatment was effective in reducing phenol levels in wastewater. SEM and FTIR analyses of the fouled membrane revealed that organic fouling is the most influential factor in flux decline. Hydrocarbon, BETX, phenol, and salts make up the foulant deposits on the membrane surface. Ozonation is also responsible for reducing the fouling resistance during PRW filtration.

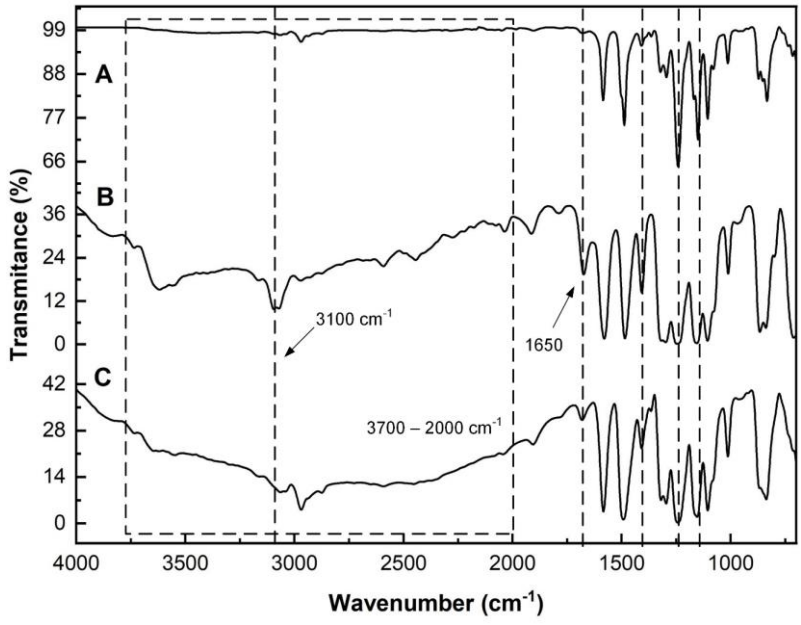

Fig. 11. FTIR spectra of (A) clean PSf-TiO_2 membrane, (B) fouled membrane with pre-ozonation, (C) fouled membrane without pre-ozonation.

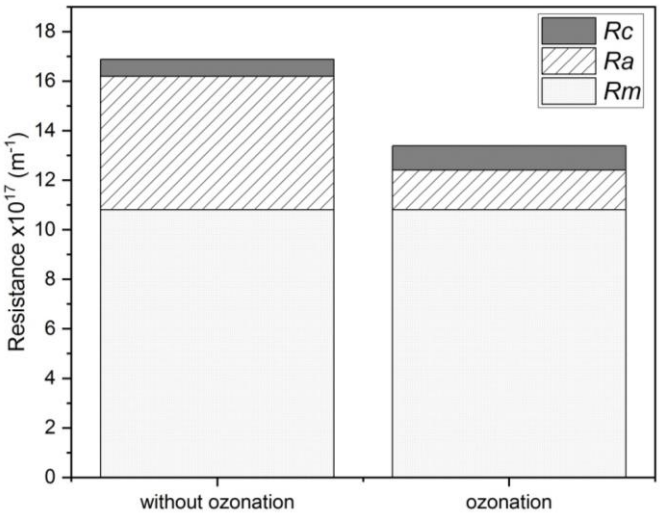

Fig. 12. Membrane resistances during petroleum wastewater treatment at 5 bar trans-membrane pressure for 150 min filtration.

Acknowledgment

This research was financially supported by the Indonesia Research, Technology, and Higher Education Ministry under the research scheme Excellent Applied Research in Higher Education (257-132/UN7.P4.3/PP/2019). The authors also would like to thank to the Department of Chemical Engineering at Diponegoro University for the use of the supporting facilities.

References

[1] A. Medel, F. Lugo, Y. Meas, Application of Electrochemical Processes for Treating Effluents from Hydrocarbon Industries, in: Electrochemical Water and Wastewater Treatment, Elsevier, 2018: pp. 365–392. https://doi.org/10.1016/B978-0-12-813160-2.00014-6.

[2] T. Al-Khalid, M.H. El-Naas, Organic Contaminants in Refinery Wastewater: Characterization and Novel Approaches for Biotreatment, in: M. Zoveidavianpoor (Ed.), Recent Insights in Petroleum Science and Engineering, InTech, 2018. https://doi.org/10.5772/intechopen.72206.

[3] A. Roy, P. Sar, J. Sarkar, A. Dutta, P. Sarkar, A. Gupta, B. Mohapatra, S. Pal, S.K. Kazy, Petroleum hydrocarbon rich oil refinery sludge of North-East India harbours anaerobic, fermentative, sulfate-reducing, syntrophic and methanogenic microbial populations, BMC Microbiol. 18 (2018) 151. https://doi.org/10.1186/s12866-018-1275-8.

[4] T. Rasheed, M. Bilal, F. Nabeel, M. Adeel, H.M.N. Iqbal, Environmentally-related contaminants of high concern: Potential sources and analytical modalities for detection, quantification, and treatment, Environ. Inter. 122 (2019) 52–66. https://doi.org/10.1016/j.envint.2018.11.038.

[5] M.H. El-Naas, S. Al-Zuhair, M.A. Alhaija, Removal of phenol from petroleum refinery wastewater through adsorption on date-pit activated carbon, Chem. Eng. J. 162 (2010) 997–1005. https://doi.org/10.1016/j.cej.2010.07.007.

[6] C.E. Santo, V.J.P. Vilar, C.M.S. Botelho, A. Bhatnagar, E. Kumar, R.A.R. Boaventura, Optimization of coagulation–flocculation and flotation parameters for the treatment of a petroleum refinery effluent from a Portuguese plant, Chem. Eng. J. 183 (2012) 117–123. https://doi.org/10.1016/j.cej.2011.12.041.

[7] R. de Abreu Domingos, F.V. da Fonseca, Evaluation of adsorbent and ion exchange resins for removal of organic matter from petroleum refinery wastewaters aiming to increase water reuse, J. Environ. Manage. 214 (2018) 362–369. https://doi.org/10.1016/j.jenvman.2018.03.022.

[8] D. Bhagawan, S. Poodari, S. Golla, V. Himabindu, S. Vidyavathi, Treatment of the petroleum refinery wastewater using combined electrochemical methods, Des. Water. Treat. 57 (2016) 3387–3394. https://doi.org/10.1080/19443994.2014.987175.

[9] G. Boczkaj, A. Fernandes, P. Makoś, Study of Different Advanced Oxidation Processes for Wastewater Treatment from Petroleum Bitumen Production at Basic pH, Ind. Eng. Chem. Res. 56 (2017) 8806–8814. https://doi.org/10.1021/acs.iecr.7b01507.

[10] M. Ebrahimi, H. Kazemi, S.A. Mirbagheri, T.D. Rockaway, An optimized biological approach for treatment of petroleum refinery wastewater, J. Environ. Chem. Eng. 4 (2016) 3401–3408. https://doi.org/10.1016/j.jece.2016.06.030.

[11] T.D. Kusworo, N. Aryanti, Qudratun, D.P. Utomo, Oilfield produced water treatment to clean water using integrated activated carbon-bentonite adsorbent and double stages membrane process, Chem. Eng. J. 347 (2018) 462–471. https://doi.org/10.1016/j.cej.2018.04.136.

[12] O.A. Fadali, E.E. Ebrahiem, T.E. Farrag, M.S. Mahmoud, A. El-Gamil, Treatment of Oily Wastewater Produced from Refinery Processes using Adsorption Technique, Minia J. Eng. Technol. 32 (2013) 15.

[13] Ş. Demırcı, B. ErdoĞan, R. Özcımder, Wastewater treatment at the petroleum refinery, Kirikkale, Turkey using some coagulants and Turkish clays as coagulant aids, Water Res. 32 (1998) 3495–3499. https://doi.org/10.1016/S0043-1354(98)00111-0.

[14] L. Yan, Y. Wang, J. Li, H. Ma, H. Liu, T. Li, Y. Zhang, Comparative study of different electrochemical methods for petroleum refinery wastewater treatment, Desalination. 341 (2014) 87–93. https://doi.org/10.1016/j.desal.2014.02.037.

[15] A.N. Azizah, I.N. Widiasa, Advanced Oxidation Processes (AOPs) for Refinery Wastewater Treatment Contains High Phenol Concentration, MATEC Web Conf. 156 (2018) 03012. https://doi.org/10.1051/matecconf/201815603012.

[16] E. Brillas, I. Sirés, M.A. Oturan, Electro-Fenton Process and Related Electrochemical Technologies Based on Fenton's Reaction Chemistry, Chem. Rev. 109 (2009) 6570–6631. https://doi.org/10.1021/cr900136g.

[17] J. Cai, X.-L. Cao, Y. Zhao, F.-Y. Zhou, Z. Cui, Y. Wang, S.-P. Sun, The establishment of high-performance anti-fouling nanofiltration membranes via cooperation of annular supramolecular Cucurbit[6]uril and dendritic polyamidoamine, J. Membr. Sci. 600 (2020) 117863. https://doi.org/10.1016/j.memsci.2020.117863.

[18] W.-J. Yang, D.-D. Shao, Z. Zhou, Q.-C. Xia, J. Chen, X.-L. Cao, T. Zheng, S.-P. Sun, Carbon quantum dots (CQDs) nanofiltration membranes towards efficient biogas slurry valorization, Chem. Eng. J. 385 (2020) 123993. https://doi.org/10.1016/j.cej.2019.123993.

[19] T.D. Kusworo, A.F. Ismail, N. Aryanti, W. Widayat, Q. Qudratun, D.P. Utomo, Enhanced anti-fouling behavior and performances of nano hybrid PES-SiO2 and PES-ZnO membranes for produced water treatment, JT. 79 (2017). https://doi.org/10.11113/jt.v79.10692.

[20] M.N. Abu Seman, M. Khayet, Z.I. Bin Ali, N. Hilal, Reduction of nanofiltration membrane fouling by UV-initiated graft polymerization technique, J. Membr. Sci. 355 (2010) 133–141. https://doi.org/10.1016/j.memsci.2010.03.014.

[21] D.M. Correia, C. Ribeiro, V. Sencadas, G. Botelho, S.A.C. Carabineiro, J.L.G. Ribelles, S. Lanceros-Méndez, Influence of oxygen plasma treatment parameters on poly(vinylidene fluoride) electrospun fiber mats wettability, Prog. Org. Coat. 85 (2015) 151–158. https://doi.org/10.1016/j.porgcoat.2015.03.019.

[22] N. Kim, D.H. Shin, Y.T. Lee, Effect of silane coupling agents on the performance of RO membranes, J. Membr. Sci. 300 (2007) 224–231. https://doi.org/10.1016/j.memsci.2007.05.039.

[23] T.D. Kusworo, Qudratun, D.P. Utomo, Indriyanti, I.R. Ramadhan, Enhancement of separation performance of nano hybrid PES –TiO2 membrane using three combination effects of ultraviolet irradiation, ethanol-acetone immersion, and thermal annealing process for CO2 removal, J. Environ. Chem. Eng. 6 (2018) 2865–2873. https://doi.org/10.1016/j.jece.2018.04.023.

[24] W. Smith, Principles of ozone generation, Watertec Engineering Pty Ltd, Australia, 2011.

[25] P. Kopf, E. Gilbert, S.H. Eberle, TiO2 photocatalytic oxidation of monochloroacetic acid and pyridine: influence of ozone, J. Photochem. Photobiol., A. 136 (2000) 163–168. https://doi.org/10.1016/S1010-6030(00)00331-2.

[26] H.C. Bidsorkhi, H. Riazi, D. Emadzadeh, M. Ghanbari, T. Matsuura, W.J. Lau, A.F. Ismail, Preparation and characterization of a novel highly hydrophilic and antifouling polysulfone/nanoporous TiO 2 nanocomposite membrane, Nanotechnology. 27 (2016) 415706. https://doi.org/10.1088/0957-4484/27/41/415706.

[27] T.D. Kusworo, D. Soetrisnanto, N. Aryanti, D.P. Utomo, Qudratun, V.D. Tambunan, N.R. Simanjuntak, Evaluation of Integrated modified nanohybrid polyethersulfone-ZnO membrane with single stage and double stage system for produced water treatment into clean water, J. Water Proc. Eng. 23 (2018) 239–249. https://doi.org/10.1016/j.jwpe.2018.04.002.

[28] T.D. Kusworo, N. Aryanti, Widayat, Qudratun, D.P. Utomo, Effect of Ultraviolet on the Morphology and Performance of PES-Nano-Silica Hybrid Membrane for Produced Water Treatment, Adv. Sci. Lett. 23 (2017) 5744–5747. https://doi.org/10.1166/asl.2017.8820.

[29] T.D. Kusworo, N. Aryanti, Qudratun, D.P. Utomo, Widayat, Improvement in nano-hybrid membrane PES–nanosilica performance using ultra violet irradiation and acetone–ethanol immersion for produced water treatment, Int. J. Environ. Sci. Technol. 16 (2019) 973–986. https://doi.org/10.1007/s13762-018-1718-7.

[30] G. Balcıoğlu, Z.B. Gönder, Baker's yeast wastewater advanced treatment using ozonation and membrane process for irrigation reuse, Process Saf. Environ. Prot. 117 (2018) 43–50. https://doi.org/10.1016/j.psep.2018.04.006.

[31] S. Huang, R.H.A. Ras, X. Tian, Antifouling membranes for oily wastewater treatment: Interplay between wetting and membrane fouling, Curr. Opin. Colloid Interface Sci. 36 (2018) 90–109. https://doi.org/10.1016/j.cocis.2018.02.002.

[32] G. Wu, S. Gan, L. Cui, Y. Xu, Preparation and characterization of PES/TiO2 composite membranes, Appl. Surf. Sci. 254 (2008) 7080–7086. https://doi.org/10.1016/j.apsusc.2008.05.221.

[33] D. Emadzadeh, W.J. Lau, T. Matsuura, M. Rahbari-Sisakht, A.F. Ismail, A novel thin film composite forward osmosis membrane prepared from PSf–TiO2 nanocomposite substrate for water desalination, Chem. Eng. J. 237 (2014) 70–80. https://doi.org/10.1016/j.cej.2013.09.081.

[34] S. Khuntia, S.K. Majumder, P. Ghosh, Removal of Ammonia from Water by Ozone Microbubbles, Ind. Eng. Chem. Res. 52 (2013) 318–326. https://doi.org/10.1021/ie302212p.

[35] J.F. Forero, J.J. Duque, F. Rios, J. Diaz, Ozone for phenol treatment in industrial wastewater, C.T.F Cienc. Tecnol. Futuro. 2 (2001) 17–26. http://www.scielo.org.co/scielo.php?script=sci_arttext&pid=S0122-53832001000100002&lng=en&nrm=iso.

[36] Y. Jung, E. Hong, M. Kwon, J.-W. Kang, A kinetic study of ozone decay and bromine formation in saltwater ozonation: Effect of O3 dose, salinity, pH, and temperature, Chem. Eng. J. 312 (2017) 30–38. https://doi.org/10.1016/j.cej.2016.11.113.

[37] E.L. Yong, Y.-P. Lin, Effects of pH value and temperature on the initiation, promotion, inhibition and direct reaction rate constants of natural organic matter in ozonation, RSC Adv. 6 (2016) 18587–18595. https://doi.org/10.1039/C5RA19359A.

[38] A.V. Levanov, O.Ya. Isaykina, N.K. Amirova, E.E. Antipenko, V.V. Lunin, Photochemical oxidation of chloride ion by ozone in acid aqueous solution, Environ. Sci. Pollut. Res. 22 (2015) 16554–16569. https://doi.org/10.1007/s11356-015-4832-9.

[39] J.M. Hales, D.R. Drewes, Solubility of ammonia in water at low concentrations, Atmos. Environ. (1967). 13 (1979) 1133–1147. https://doi.org/10.1016/0004-6981(79)90037-4.

[40] T. Ye, W. Chen, H. Xu, N. Geng, Y. Cai, Preparation of TiO2/graphene composite with appropriate N-doping ratio for humic acid removal, J. Mater. Sci. 53 (2018) 613–625. https://doi.org/10.1007/s10853-017-1509-4.

[41] X. Zuo, L. Wang, J. He, Z. Li, S. Yu, SEM-EDX studies of SiO2/PVDF membranes fouling in electrodialysis of polymer-flooding produced wastewater: Diatomite, APAM and crude oil, Desalination. 347 (2014) 43–51. https://doi.org/10.1016/j.desal.2014.05.020.

[42] A. Lim, Membrane fouling and cleaning in microfiltration of activated sludge wastewater, J. Membr. Sci. 216 (2003) 279–290. https://doi.org/10.1016/S0376-7388(03)00083-8.

[43] S. Jiang, Y. Li, B.P. Ladewig, A review of reverse osmosis membrane fouling and control strategies, Sci. Tot. Environ. 595 (2017) 567–583. https://doi.org/10.1016/j.scitotenv.2017.03.235.

[44] H.Z. Shafi, A. Matin, S. Akhtar, K.K. Gleason, S.M. Zubair, Z. Khan, Organic fouling in surface modified reverse osmosis membranes: Filtration studies and subsequent morphological and compositional characterization, J. Membr. Sci. 527 (2017) 152–163. https://doi.org/10.1016/j.memsci.2017.01.017.

[45] C.H. Kuo, H.S. Soong, Oxidation of benzene by ozone in aqueous solutions, Chem. Eng. J. 28 (1984) 163–171. https://doi.org/10.1016/0300-9467(84)85052-2.